PAPER

Check for updates

Unifying lipolysis under intestinal INFOGEST conditions by total surface area and coalescence

Lingfeng Wu, Meinou Corstens, ID * Ameer Khan Patan, Boxin Deng ID and Karin Schroën

The INFOGEST *in vitro* digestion protocol is an important step toward quantifiable comparison of lipid digestion results. Still, interpreting results across different food emulsions remains challenging due to differences in oil content, droplet size, and emulsion stability. Because of that, we systematically investigated whey protein isolate-stabilized emulsions (d_{32} = 0.16 and 7.2 μm) at 0.28–56.35 mM oil concentration, and considered lipase and bile salt levels as additional factors. As expected, smaller droplets digested faster than larger ones at the same oil concentration, but differences could not be explained by available surface area alone. We found that lipolysis was governed by the interplay between oil content, droplet size, emulsion stability, and enzyme availability. We developed a lipolysis-coalescence model that incorporates a critical total surface area (C_{TSA}), below which the whole surface area contributes to lipolysis, while this is limited to the critical total surface area when enzymes are present in surplus. Besides, a coalescence rate constant is introduced, which reduces the available surface area, in conjunction with a droplet size decrease due to digestion, and thus limiting the rate (and extent) of lipolysis in time. The model was used to compare digestive conditions with varying amounts of lipase and bile, and was able to capture essential effects. Our lipolysis-coalescence model can be used to deconvolute the effects of droplet size, initial oil concentration and coalescence on lipolysis, which is the essential step needed to arrive at a unified interpretation of lipid digestion under INFOGEST conditions.

1. Introduction

Lipids are essential to human health, providing energy and nutrients, with plant oil providing additional benefits, such as antioxidant[1] and anti-inflammation activities.[2] However, when eaten in high amounts and/or digested rapidly, lipid digestion may lead to adverse health effects such as overweight, obesity,[3] hyperglycaemia, and hyperlipidaemia.[4] Controlling the rate and extent of lipid digestion is essential for creating desirable effects, such as inducing satiety for anti-obesity strategies.[5–7]

To investigate digestion in the gastrointestinal (GI) tract, *in vivo* methods (animal and human) have been used, but these methods are time-consuming, costly and come with ethical constraints.[8] For this reason, *in vitro* digestion models were developed, also to gain mechanistic understanding of food digestion.[8–11] To improve comparability between labs, static *in vitro* digestion conditions were standardized in 2014,[12] and updated in 2019 in the harmonized INFOGEST 2.0 protocol.[13] This protocol is nowadays widely used to evaluate the lipolysis

Wageningen University, Department of Agrotechnology & Food Sciences, Laboratory of Food Process Engineering Group, Bornse Weilanden 9, 6708 WG Wageningen, The Netherlands. E-mail: meinou.corstens@wur.nl

products (*e.g.* release of free fatty acids (FFA)) of various food systems: oils,[1] emulsions,[14] emulsion-gels[15,16] and oleogels.[17]

In the static INFOGEST 2.0 protocol, the lipolytic activity and bile salt concentration are set to mimic the intestinal digestion.[18,19] Various interactive effects have been reported for enzymes and bile. Bile salts support the adsorption of co-lipase and lipase, and help solubilise and thus release the lipolysis products accumulated at the interface.[19] A higher concentration of both lipase and bile salts has been reported to largely accelerate the rate and extent of lipolysis.[20,21] To be complete, inhibition effects from particular concentrations onwards have been reported to reduce lipid digestion.[22,23]

Since lipolysis is an interfacial reaction, the substrate concentration should be described in terms of available interfacial area. This is not the case in the INFOGEST protocol, in which a standard amount of food sample is used, and does not consider *e.g.*, the amount of oil, the droplet size, and certainly not droplet coalescence. However, these factors together determine available substrate and hence, lipolysis kinetics under the fixed enzymatic conditions of the protocol. Some effects have also been reported in literature. For instance, a high amount of oil leads to a lower degree of lipolysis.[24–26] Besides, the intestinal lipolysis rate[27] and total extent of lipid digestion[28] has been reported to increase with decreasing oil droplet size, indicating that total interfacial

area is important.[29] Furthermore, it was noted that coalescence largely reduced the interfacial area and intestinal lipolysis rate.[30–32] In essence, all the individual aspects have been touched upon, but they have never been considered as a 'total package' to describe lipolysis quantitatively.

On top of effects contributing to the total surface area available, the reaction kinetics need to be incorporated properly. Lipolysis curves have been fitted with first-order kinetics,[21,33,34] but the obtained lipolysis rate constant and final lipolysis extent cannot be related to the changing total surface area. Okuro et al.,[35] reported that the final lipolysis extent decreased with increasing oil concentration following a logarithmic trend but other effects were also reported.[36–38]

The approach that we take in this paper is that initially, the available total surface area is determined by the amount of oil present, and the droplet size, and that during digestion, the surface area is reduced through two effects: 1. The action of the enzyme (reducing the droplet size), and 2. Coalescence of droplets (increasing the droplet size). In the current study, we aim to quantitatively describe the effect of total surface area of oil droplets on intestinal lipolysis under INFOGEST conditions. We systematically vary the amount of oil and the size of the droplets (i.e., specific surface area), and take droplet coalescence into account. We predict lipolysis (FFA release) using a reaction rate constant defined on m^2-basis, in conjunction with a first order coalescence model. The results obtained, lead to detailed understanding of lipolysis under INFOGEST in vitro digestion conditions, highlighting the exact effect of surface area therein, and thus the importance of emulsion stability for fatty acid release.

2. Materials and methods

2.1. Materials

Safflower oil was purchased from De Wit Specialty oils (19200 Safflower Oil High Linoleic Refined, The Netherlands). Whey protein isolate was supplied by Davisco Foods International (BiPro, Eden Prairie, Minnesota, USA; purity 97.5%). Sodium phosphate monobasic, sodium phosphate dibasic, calcium chloride dihydrate, sodium chloride, sodium hydroxide, magnesium chloride, potassium phosphate monobasic, pancreatin from porcine pancreas (P7545), lipase from porcine pancreas (L3126) and porcine bile bovine (B3883) were obtained from Sigma Aldrich (St Louis, MO, USA). Potassium chloride, monopotassium phosphate were provided by VWR International (Radnor, PA, USA). All chemicals were used as received. Milli-Q water (Millipore Milli-Q system, Q-POD with Millipak Express 40-0.22 μm filter, Merck Millipore, USA) was used throughout this study.

2.2. Method

2.2.1. Preparation of emulsions

Micrometre-sized (large) emulsion. Whey protein isolate (WPI, 0.5 wt%) was added to phosphate buffer (10 mM, pH 7.0) and stirred until dissolved. Safflower oil (weight ratio to WPI solution at 1 : 9) was added to this solution and homogenized

using a rotor-stator homogenizer (Ika T18 basic Ultra-Turrax homogenizer, Staufen, Germany) for 5 min at 10 000 rpm to obtain emulsions with an average size of 7.2 μm (d_{32}).

Nanometre-sized (small) emulsion. The micrometre-sized emulsion described above was emulsified further (Microfluidiser, chamberF12Y and APM H30Z, Microfluidics, Massachusetts, USA) leading to an emulsion with an average size of 0.16 μm (d_{32}) after 3 passes at 280 kPa.

Droplet size measurement. The droplet size of the emulsions was measured using static light scattering (Mastersizer 3000 with Hydro SM dispersion unit, Malvern Instruments Ltd, Malvern, UK). The refractive index of the safflower oil was set at 1.46 (with an absorption index of 0.001) and that of the dispersant at 1.33.

2.2.2. In vitro digestion (INFOGEST).
The INFOGEST conditions in our work only refer to the recommended conditions of simulated intestinal digestion, so without oral and gastric phases. We made this choice to ensure a well-defined initial state (droplet size), and prevent oro-gastric instability or pre-lipolysis to over-complicate the fundamental modelling study we intend to conduct. The total volume of digestion was 20 mL (the addition of NaOH was ignored), and the range of intestinal oil concentrations was 0.28–56.35 mM. The simulated intestinal fluid (SIF) was adjusted to always have electrolyte concentrations in the digestive system of 6.8 mM KCl, 0.33 mM $MgCl_2$, 123.4 mM NaCl, 0.6 mM $CaCl_2$, 0.8 mM KH_2PO_4 based on INFOGEST protocol.[13] Pancreatin, lipase and bile salts were dissolved in a stock solution and added to obtain a lipase activity of 2000 U mL^{-1} (or 200 U mL^{-1} when indicated) and bile salt concentration of 10 mM (or 5 mM when indicated). The intestinal incubation was done at 37.0 °C for 10 min at pH 7.0 using a pH-stat (Metrohm 877 Titrino plus, Schiedam, The Netherlands) and stirred at 240 rpm.[16]

The initial lipolysis rate (< 30 s) was determined from the 'linear' part of the curve using eqn (1):

$$\text{(Initial) lipolysis rate} = \frac{\Delta V_{\text{NaOH}} \times N_{\text{NaOH}} \times 1000}{\Delta t \times V_{\text{total}}} \quad (1)$$

The lipolysis rate is expressed as free fatty acid released (μmol mL^{-1} s^{-1}), with V_{NaOH} the titrated volume NaOH (mL), N_{NaOH} the molar concentration of NaOH (M), t the time (s, in the 'linear' part of the curve) and the total volume of digestion (V_{total}, 20 mL). Since the WPI concentration is low in the digesta, we safely ignored its effect on the calculation of FFA release (as confirmed with a blank measurement). The percentage of released free fatty acid is calculated[33,39] (assuming that 2 fatty acids are released per lipid; eqn (2)), with MW_{lipid} the average molecular weight of the lipids (874 g mol^{-1}), and m_{lipid} the mass of lipid used (g):

$$\text{FFA release (\%)} = \frac{V_{\text{NaOH}} \times N_{\text{NaOH}} \times MW_{\text{lipid}}}{2m_{\text{lipid}}} \times 100\% \quad (2)$$

2.2.3. Lipolysis kinetics model
Initial parameters. The amount of surface area available in the digestive liquid follows from the specific surface area of

the emulsion ($m^2\ m^{-3}$) defined by volume proportion (φ) and size of droplet (d_{drop}):

$$A_{spec} = \frac{6 \times \varphi}{d_{drop}} \quad (3)$$

The total surface area available (TSA, $m^2\ mL^{-1}$) in the emulsion added to the digestive fluid was calculated using eqn (4):

$$TSA = \frac{A_{spec} \times V_{emulsion}}{V_{total}} \quad (4)$$

With $V_{emulsion}$ the emulsion volume added to the digestive liquid (m^3). Depending on how much lipase is present, the available total surface area will either be saturated with lipase, or be partly uncovered. This transition takes place at a critical total surface area in the digestive system (C_{TSA}, $m^2\ mL^{-1}$, please note that this is not the specific surface area), which determines the lipolysis rate (LR, $\mu mol\ mL^{-1}\ s^{-1}$) as follows:

$$At\ TSA\ <\ C_{TSA}:\ LR = k_{lipolysis} \times TSA \quad (5)$$

$$At\ TSA\ >\ C_{TSA}:\ LR = k_{lipolysis} \times C_{TSA} \quad (6)$$

The lipolysis rate constant ($k_{lipolysis}$) is defined in $\mu mol\ m^{-2}\ s^{-1}$. Due to lipolysis, and subsequent removal of fatty acids, the droplet size reduces thus reducing the available surface area. When coalescence occurs, the available surface area also reduces, for which we use the following first order equation:

$$N_t = N_0 \times e^{-k_{coal} \times t} \quad (7)$$

With N_t the number of droplets, N_0 the initial number of droplets calculated by the ratio of volume of oil to volume of single oil droplet ($V_{oil}/V_{droplet}$), k_{coal} the coalescence rate constant (s^{-1}). Both effects are discussed in detail in the results section. The amount of released fatty acids are calculated from the residual amount of oil ($M_{oil(t)}$, μmol) compared to the initial amount of oil ($M_{oil(0)}$, μmol):

$$FFA\ released_t\ (\%) = \left(1 - \frac{M_{oil(t)}}{M_{oil(0)}}\right) \times 100\% \quad (8)$$

The algorithm used to describe the percentage release of FFA and to compare with the experimental values at any time can be found in Fig. S1. The model in the following sections means the mathematical model including lipolysis and coalescence.

2.2.4. Statistical analysis. Microsoft® Excel® Office 365 (Redmond, Washington, USA) was used to determine the initial linear slope (*i.e.*, measured initial lipolysis rate) for each experiment, and other data analysis. Matlab R2023b was used to fit the FFA release model, featuring the lipolysis rate constant, the coalescence rate constant, and the critical total surface area. Origin 2024 was used to generate the figures. For significance, SPSS 28 (IBM, Armonk, New York, USA) was used with one-way ANOVA with Turkey's *post-hoc* test. Droplet size measurement and *in vitro* digestion were done in triplicate.

3. Results and discussion

3.1. Lipolysis as function of oil concentration and droplet size

Under the INFOGEST conditions of simulated intestinal digestion (lipase activity of 2000 U mL^{-1}, 10 mM bile salts), and using the same amount of oil, emulsions with small droplets (0.16 μm) had a considerably higher initial lipolysis rate than large droplets (7.2 μm) (Fig. 1A). The initial lipolysis rate of emulsions with large droplets seems to increase linearly with

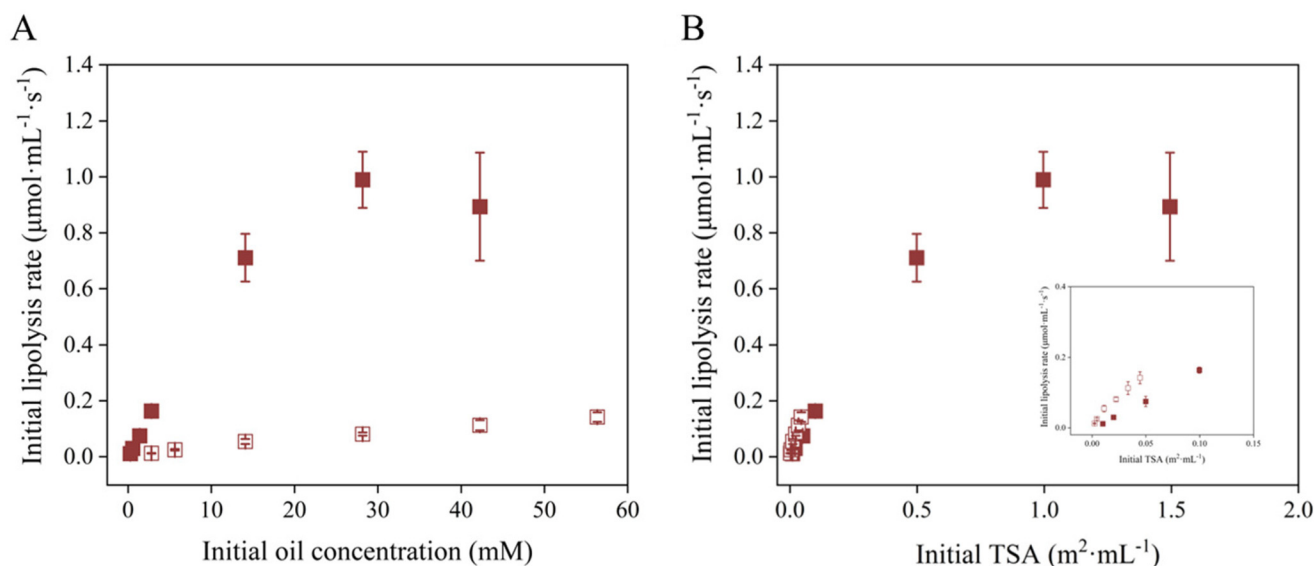**Fig. 1** (A) Effect of initial oil concentration on initial lipolysis rate of small and large emulsion droplets (0.16 and 7.2 μm, filled and empty symbols, respectively) under INFOGEST conditions. Mean values with standard deviations are shown (*n* = 3). (B) The same data now expressed per available initial surface area (with zoomed insert).

oil concentration. For small droplets, this is the case at low oil concentration, after which the initial lipolysis rate levels off at higher oil concentration. The difference in initial total surface area between the two emulsions is ~40 times, and when replotting the data as function of initial surface area, as illustrated in Fig. 1B, it is clear that these lines may seem close but do not coincide. Most obvious is that at high surface area, the lipolysis will be limited by the total surface area, leading to a 'plateau' for the small droplets. This indicates that the lipolysis rate of emulsions is determined by the critical total surface area under fixed intestinal conditions. The initial slopes of the curves are also different, which could be indicative of different coalescence rates. Extensive coalescence was observed already after 1 minute of digestion. These observations indicate that various effects play a role in these experiments.
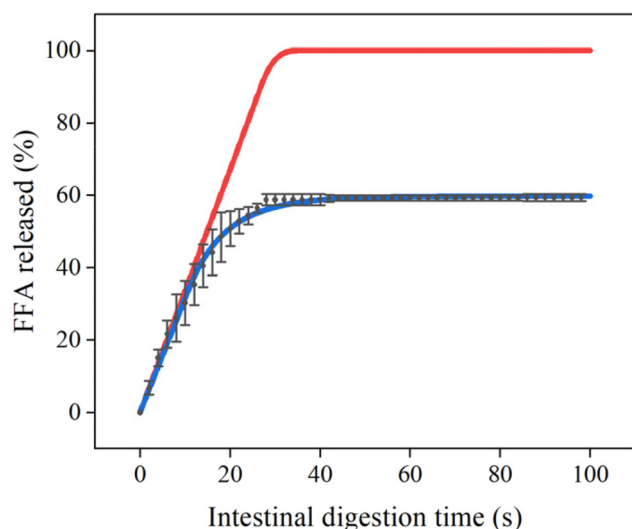

Fig. 2 Prediction of FFA release based on the combined lipolysis-coalescence model (blue line), and lipolysis only (red line) for small oil droplets at an initial oil concentration of 14 mM (data shown as black dots).

3.2. Coalescence and lipolysis kinetics

In order to illustrate the effect of coalescence on lipolysis early on, in Fig. 2, measured data (small oil droplets at an initial oil concentration of ~14 mM) is compared to scenarios based on lipolysis only (red line) and one that includes coalescence (blue line) (both lines are generated with the model taking a critical total surface area into account, as discussed later). After 30 s, a plateau is reached with approximately 60% of FFAs released, which clearly shows that coalescence plays an important role in these experiments, both initially and in line with the plateaus,[35] that otherwise would not be surpassed (as happens in the red line).

The overall lipolysis-coalescence model is used to describe the fatty acid release pattern of emulsions with small droplets, using the fitting procedure described in 'methods' (algorithm in Fig. S1). This allowed us to determine the lipolysis rate constant and critical total surface area under INFOGEST conditions, as well as the coalescence rate constants, as shown in Table 1 (all fits are given in Fig. S2). The lipolysis rate constant ($k_{lipolysis}$) was 8.5 µmol m^{-2} s^{-1} for small droplets, and the critical total surface area (C_{TSA}) 0.11 m^2 mL^{-1}. This implies that the lipolysis rate increases linearly with the surface area when below 0.11 m^2 mL^{-1}, while at higher surface areas the lipolysis rate is constant at 0.935 µmol mL^{-1} s^{-1}, as illustrated in Fig. 3. When replotting this data as lipolysis rate per area and time, and using the same x-axis, it is clear that below the critical total surface area, that the surface related lipolysis rate is constant, while it drops at higher surface area, simply because not all of the surface area can be covered with enzyme (Fig. 3).

For the larger droplets, we found a slightly lower lipolysis rate constant of 5.4 µmol m^{-2} s^{-1} (Table 1). Differences in the size distribution of both emulsions may contribute to this, but it does not explain incomplete digestion; which was probably caused by coalescence. When focusing on the coalescence rate constants in Table 1, it is clear that the k_{coal}-values for large emulsion droplets are significantly smaller than those for small droplets (Table 1). Most probably, the collision probability of small emulsion droplets is much higher since they

Table 1 Fitting results under INFOGEST conditions

	Initial oil concentration (mM)	Initial total surface area ($t = 0$) (m^2 mL^{-1})	Lipolysis rate constant ($k_{lipolysis}$) (µmol m^{-2} s^{-1})	Critical total surface area (C_{TSA}) (m^2 mL^{-1})	Coalescence rate constant (k_{coal}) (s^{-1})	Calculated initial lipolysis rate ($t = 0$) (µmol mL^{-1} s^{-1})
Large emulsion droplets (7.2 µm)	2.82	0.0022	**5.4**	**0.11**	0.0074 ± 0.0048a	0.019
	5.64	0.0045			0.0038 ± 0.0038a	0.038
	14.09	0.0111			0.018 ± 0.005a	0.095
	28.18	0.0223			0.036 ± 0.004a	0.189
	42.26	0.0334			0.039 ± 0.009a	0.284
	56.35	0.0445			0.044 ± 0.004a	0.378
Small emulsion droplets (0.16 µm)	1.41	0.0498	**8.5**		0.444 ± 0.067c	0.423
	2.82	0.0996			0.476 ± 0.013c	0.847
	14.09	0.4982			0.350 ± 0.010b	0.935
	28.18	0.9964			0.267 ± 0.005b	0.935
	42.26	1.4946			0.307 ± 0.072b	0.935

Lowercase letters present a significant difference within the INFOGEST digestive condition following one-way ANOVA with Turkey's *post-hoc* test.
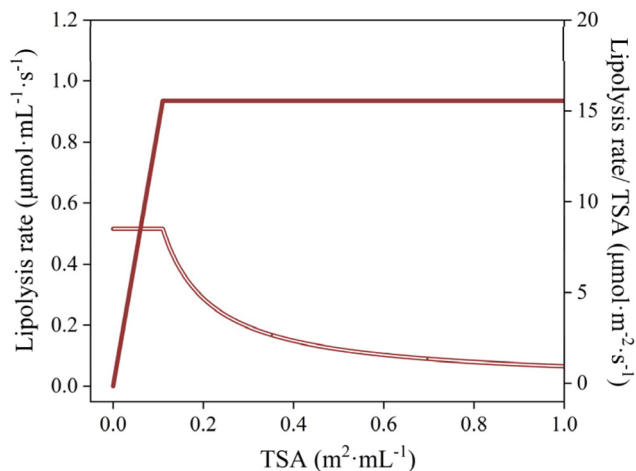
Fig. 3 Volumetric (left y axis, single line) and surface area related (right y axis, double line) lipolysis rate as function of available total surface area (TSA) during intestinal digestion under INFOGEST conditions.

are always in closer proximity due to their much higher number than their larger counterparts,[40] as seems to be occurring in the data for large droplets at higher concentration (implying closer proximity).

For small oil droplets at initial TSA > C_{TSA}, the coalescence rate constant seems to decrease. This decrease may indicate that droplets covered with lipase have a higher likelihood of coalescence. Essentially, the emulsifier initially present is displaced by components that are less able to stabilize the interface, which may result in less stable droplets.[41]

To demonstrate the relative effect of lipolysis and coalescence on the surface area over time, we made Fig. 4 for small and large droplets at an initial oil concentration of ~14 mM. Firstly, the lipolysis rate constant, critical surface area and

coalescence rate constant were obtained by using the model mentioned above (Fig. S1). We used the lipolysis-coalescence model to create the lines for two scenarios: either lipolysis ($k_{coal} = 0$), or coalescence only ($k_{lipolysis} = 0$). For both droplet sizes, the reduction in total surface areas due to coalescence is much stronger than that caused by the lipolysis reaction. We are impressed by the magnitude and effect of coalescence on lipolysis, even at such short time scales, which signifies its relevance in interpreting data from literature.

3.3. Effect of lipase activity and bile salts concentration on lipolysis kinetics

To better understand the effect of INFOGEST conditions on lipolysis, we measured lipolysis and used the model to describe varying lipase activity and bile salt concentration, following established conditions.[42] The $k_{lipolysis}$, k_{coal}, and C_{TSA} values were determined for emulsions with small droplets (to include the critical total surface area relative to the amount of enzyme present).

The lipolysis rate constants do not seem to be affected much by the bile salt concentration, but decrease by approximately half when lipase activity is reduced tenfold (Table 2). This was rather unexpected, but may be related to the coalescence behaviour discussed later. The fitted critical total surface areas are higher for the 10-times higher lipase concentration, as would be expected, albeit that the difference is typically only a factor of 3, which may be caused by instability differences between emulsions. There is a systematic difference at low bile concentration, which may indicate that the collaborative effect between lipase and bile can be interpreted in terms of higher and lower limiting surface area, and thus faster/slower digestion.[21,43]

As mentioned previously, coalescence may have been the root cause for some of the differences in Table 2, so now we
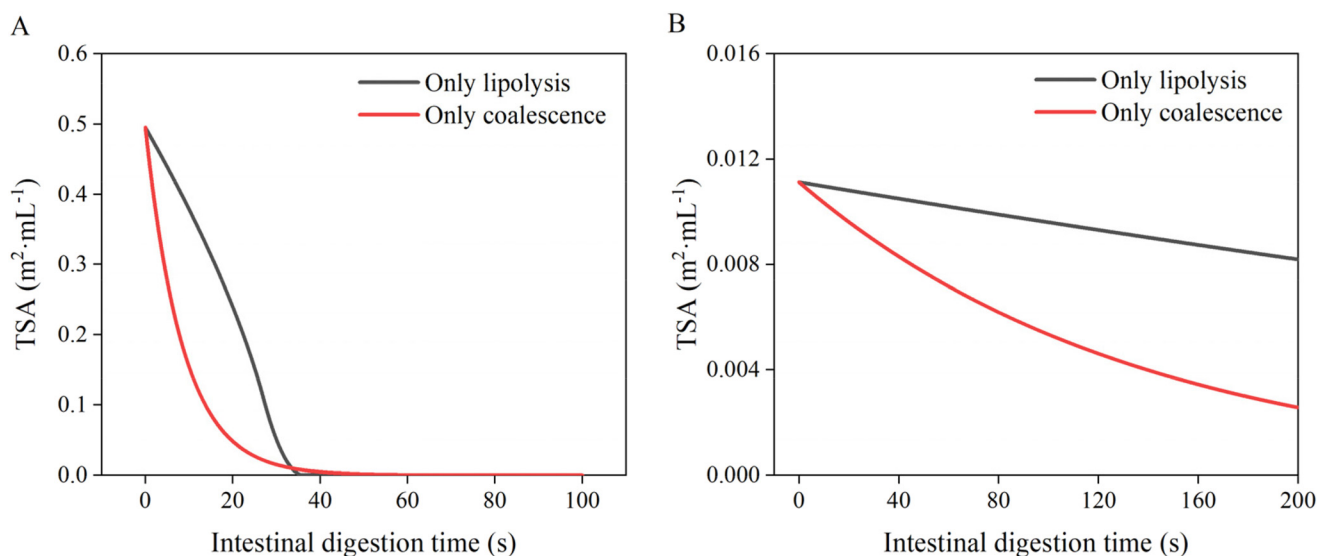
Fig. 4 Modelling the change of total surface area (TSA) due to lipolysis (black line) and coalescence (red line) during intestinal digestion of emulsions with small (A) and large (B) droplets under INFOGEST conditions at an initial oil concentration of ~14 mM.

Table 2 Fitted lipolysis rate constants (μmol m^{-2} s^{-1}, left), and critical total surface area (m^2 mL^{-1}, right) under different lipase activities and bile salt concentrations for small emulsion droplets

Bile salts concentration	Lipase activity			
	$k_{lipolysis}$ (μmol m^{-2} s^{-1})		C_{TSA} (m^2 mL^{-1})	
	2000 U mL^{-1}	200 U mL^{-1}	2000 U mL^{-1}	200 U mL^{-1}
10 mM	8.5	3.3	0.11	0.04
5 mM	8.4	4.3	0.065	0.025

focus on the fitted coalescence rate constants (see Table 3). When the model is used at low initial oil concentrations, it is very hard to determine accurate coalescence constants, if at all. The coalescence rate constants found seem to be following similar trends as mentioned before within one digestive condition. As described earlier for standard INFOGEST conditions, k_{coal}-values of emulsions with large droplets seem to increase with initial TSA, while for small emulsion droplets the k_{coal}-values seem to level off at different plateau values, depending on the lipase and bile salt concentration used, which stresses the collaborative effect of these components.[44] The bile concentration does not seem to have an effect on k_{coal}-values when lipase is used at high concentration. At low lipase activity, and for large droplets, a low bile salt concentration seems to lead to higher instability, again pointing to a delicate balance between these two components in relation to emulsion destabilisation. In general, our lipolysis-coalescence model highlighted the importance of coalescence during emulsion digestion, which makes the model suited for fast analysis of the lipolysis profile of emulsions.

In future work, the impact of gastric lipase should be systematically investigated, as it likely influences both the rate of lipolysis and droplet coalescence.[45] Quantifying this influence is challenging using conventional static *in vitro* digestion models, so a microfluidic approach could be used to enable real-time tracking of individual lipid droplets.[30] In parallel,

destabilization and re-emulsification could be described based on a dynamic digestion system with more accurate gastrointestinal shear conditions. We will then also consider the concentration[46] and type of emulsifier,[41,47] lipid type, and polyelectrolytes[23,48] to disentangle their effects on rate of lipolysis and coalescence. We expect the lipolysis-coalescence model to be instrumental in further unifying lipolysis studies in the future, and leading to clues for food emulsion design related to specific fatty acid release.

4. Conclusion

The total surface area of emulsions, and the reduction thereof, was confirmed to be the dominating factor in lipolysis under *in vitro* INFOGEST intestinal digestion. The actual lipolysis rate is highly determined by the coalescence of droplets, more than by the effect of the reaction itself, as we showed for WPI-stabilized emulsions. It is expected that interfacial displacement of the emulsifier by digestive components greatly contributes to coalescence. The experiments that were carried out at various oil concentrations, droplet sizes, and lipase and bile concentrations could all be described with a model that revolves around the lipolysis reaction rate constant, the coalescence rate constant, and a critical total surface area. The model is instrumental in mechanistically understanding intestinal lipolysis, and can be used to deconvolute various effects to arrive at a more unified understanding.

Author contributions

Lingfeng Wu: investigation, methodology, software, formal analysis, writing, Meinou Corstens: methodology, conceptualization, supervision, writing, Ameer Khan Patan: methodology, software, formal analysis, writing, Boxin Deng: investigation, writing, Karin Schroen: methodology, conceptualization, supervision, writing.

Table 3 Fitted coalescence rate constant (k_{coal}) of emulsions under different conditions

	Initial oil concentration (mM)	Initial of total surface area ($t = 0$) (m^2 mL^{-1})	2000 U mL^{-1} – 10 mM (s^{-1})	2000 U mL^{-1} – 5 mM (s^{-1})	200 U mL^{-1} – 10 mM (s^{-1})	200 U mL^{-1} – 5 mM (s^{-1})
Large emulsion droplets (7.2 μm)	1.41	0.0011	—	0.024 ± 0.018a	—	—
	2.82	0.0022	0.0074 ± 0.0048aA	0.015 ± 0.003aA	0.0021 ± 0.0036aA	0.040 ± 0.037aA
	5.64	0.0045	0.0038 ± 0.0038aA	0.009 ± 0.012aA	0.018 ± 0.006aA	0.040 ± 0.058aA
	14.09	0.0111	0.018 ± 0.005aA	0.030 ± 0.004aA	0.023 ± 0.008aA	0.179 ± 0.050bB
	28.18	0.0223	0.036 ± 0.004aA	0.054 ± 0.001aAB	0.056 ± 0.014abB	0.183 ± 0.005bC
	42.26	0.0334	0.039 ± 0.009aA	0.073 ± 0.013abA	0.068 ± 0.008abA	0.202 ± 0.028bB
	56.35	0.0445	0.044 ± 0.004a	—	—	—
Small emulsion droplets (0.16 μm)	1.41	0.0498	0.444 ± 0.067cB	0.456 ± 0.077cB	0.104 ± 0.091abA	0.225 ± 0.057bA
	2.82	0.0996	0.476 ± 0.013cA	0.337 ± 0.228cA	0.227 ± 0.037cA	0.188 ± 0.015bA
	14.09	0.4982	0.350 ± 0.010bB	0.357 ± 0.103cB	0.143 ± 0.010bcA	0.206 ± 0.023bA
	28.18	0.9964	0.267 ± 0.005bC	0.307 ± 0.044bcC	0.110 ± 0.007abA	0.181 ± 0.007bB
	42.26	1.4946	0.307 ± 0.072bB	0.359 ± 0.096cB	0.084 ± 0.073abA	0.193 ± 0.016bAB

Lowercase letters or uppercase letters present a significant difference within the group of same digestive condition or within the same initial TSA following one-way ANOVA with Turkey's *post-hoc* test, respectively.

Conflicts of interest

There are no conflicts to declare.

Data availability

The data has been published by WUR library as: https://doi.org/10.17887/WUR01-H3MJ5F.

Supplementary information (SI) is available. It contains the algorithm of model and the fitting results. All the details can be found in the dataset above. See DOI: https://doi.org/10.1039/d5fo03083h.

Acknowledgements

References

1 A. S. Salsinha, S. A. Cunha, M. Machado, L. M. Rodríguez-Alcalá, J. B. Relvas and M. Pintado, Assessment of the bioaccessibility and bioavailability prediction of omega 3 and conjugated fatty acids by *in vitro* standardized digestion model (INFOGEST) and cell model, *Food Biosci.*, 2023, **53**, 102635.

2 A. S. Salsinha, L. M. Rodríguez-Alcalá, J. B. Relvas and M. E. Pintado, Fatty acids role on obesity induced hypothalamus inflammation: From problem to solution – A review, *Trends Food Sci. Technol.*, 2021, **112**, 592–607.

3 F. Lopez-Jimenez, W. Almahmeed, H. Bays, A. Cuevas, E. Di Angelantonio, C. W. le Roux, N. Sattar, M. C. Sun, G. Wittert, F. J. Pinto and J. P. H. Wilding, Obesity and cardiovascular disease: mechanistic insights and management strategies. A joint position paper by the World Heart Federation and World Obesity Federation, *Eur. J. Prev. Cardiol.*, 2022, **29**, 2218–2237.

4 World Health Organization, *World Health Statistics 2023 Monitoring health for the SDGs Sustainable Development Goals HEALTH FOR ALL*, World Health Organization, 2023.

5 J. Wilbrink, G. Masclee, T. Klaassen, M. van Avesaat, D. Keszthelyi and A. Masclee, Review on the regional effects of gastrointestinal luminal stimulation on appetite and energy intake: (Pre)clinical observations, *MDPI AG*, 2021, preprint, DOI: 10.3390/nu13051601.

6 K. Schroën, L. Wu and M. Corstens, Food-grade microgel capsules tailored for anti-obesity strategies through microfluidic preparation, *Curr. Opin. Food Sci.*, 2022, **45**, 100816.

7 M. N. Corstens, F. J. Troost, A. M. E. Alleleyn, T. Klaassen, C. C. Berton-Carabin, K. Schroën and A. A. M. Masclee, Encapsulation of lipids as emulsion-alginate beads reduces food intake: a randomized placebo-controlled cross-over human trial in overweight adults, *Nutr. Res.*, 2019, **63**, 86–94.

8 S. J. Hur, B. O. Lim, E. A. Decker and D. J. McClements, *In vitro* human digestion models for food applications, *Food Chem.*, 2011, **125**, 1–12.

9 F. Kong and R. P. Singh, A Model Stomach System to Investigate Disintegration Kinetics of Solid Foods during Gastric Digestion, *J. Food Sci.*, 2008, **73**, E202–E210.

10 K. S. Kulp, S. L. Fortson, M. G. Knize and J. S. Felton, An *in vitro* model system to predict the bioaccessibility of heterocyclic amines from a cooked meat matrix, *Food Chem. Toxicol.*, 2003, **41**, 1701–1710.

11 M. Beysseriat, E. A. Decker and D. J. McClements, Preliminary study of the influence of dietary fiber on the properties of oil-in-water emulsions passing through an *in vitro* human digestion model, *Food Hydrocolloids*, 2006, **20**, 800–809.

12 M. Minekus, M. Alminger, P. Alvito, S. Ballance, T. Bohn, C. Bourlieu, F. Carrière, R. Boutrou, M. Corredig, D. Dupont, C. Dufour, L. Egger, M. Golding, S. Karakaya, B. Kirkhus, S. Le Feunteun, U. Lesmes, A. MacIerzanka, A. MacKie, S. Marze, D. J. McClements, O. Ménard, I. Recio, C. N. Santos, R. P. Singh, G. E. Vegarud, M. S. J. Wickham, W. Weitschies and A. Brodkorb, A standardised static *in vitro* digestion method suitable for food – an international consensus, *Food Funct.*, 2014, **5**, 1113–1124.

13 A. Brodkorb, L. Egger, M. Alminger, P. Alvito, R. Assunção, S. Ballance, T. Bohn, C. Bourlieu-Lacanal, R. Boutrou, F. Carrière, A. Clemente, M. Corredig, D. Dupont, C. Dufour, C. Edwards, M. Golding, S. Karakaya, B. Kirkhus, S. Le Feunteun, U. Lesmes, A. Macierzanka, A. R. Mackie, C. Martins, S. Marze, D. J. McClements, O. Ménard, M. Minekus, R. Portmann, C. N. Santos, I. Souchon, R. P. Singh, G. E. Vegarud, M. S. J. Wickham, W. Weitschies and I. Recio, INFOGEST static *in vitro* simulation of gastrointestinal food digestion, *Nat. Protoc.*, 2019, **14**, 991–1014.

14 Y. Tan, Z. Zhang, J. M. Mundo and D. J. McClements, Factors impacting lipid digestion and nutraceutical bioaccessibility assessed by standardized gastrointestinal model (INFOGEST): Emulsifier type, *Food Res. Int.*, 2020, **137**, 109739.

15 D. J. L. Mat, S. Le Feunteun, C. Michon and I. Souchon, *In vitro* digestion of foods using pH-stat and the INFOGEST protocol: Impact of matrix structure on digestion kinetics of macronutrients, proteins and lipids, *Food Res. Int.*, 2016, **88**, 226–233.

16 L. Wu, K. Schroën and M. Corstens, Structural stability and release properties of emulsion-alginate beads under gastrointestinal conditions, *Food Hydrocolloids*, 2024, **150**, 109702.

17 S. Sabet, S. J. Kirjoranta, A. M. Lampi, M. Lehtonen, E. Pulkkinen and F. Valoppi, Addressing criticalities in the

INFOGEST static *in vitro* digestion protocol for oleogel analysis, *Food Res. Int.*, 2022, **160**, 111633.

18 M. Armand, Lipases and lipolysis in the human digestive tract: Where do we stand?, *Curr. Opin. Clin. Nutr. Metab. Care*, 2007, **10**, 156–164.

19 P. J. Wilde and B. S. Chu, Interfacial & colloidal aspects of lipid digestion, *Adv. Colloid Interface Sci.*, 2011, **165**, 14–22.

20 Y. Li, M. Hu and D. J. McClements, Factors affecting lipase digestibility of emulsified lipids using an *in vitro* digestion model: Proposal for a standardised pH-stat method, *Food Chem.*, 2011, **126**, 498–505.

21 D. Michels, S. H. E. Verkempinck, A. Panozzo, K. Vermeulen, M. E. Hendrickx, L. Thijs and T. Grauwet, Importance of adapted digestion conditions to simulate *in vitro* lipid digestion of broilers in different life stages, *Anim. Nutr.*, 2023, **12**, 151–158.

22 J. Maldonado-Valderrama, P. Wilde, A. MacIerzanka and A. MacKie, The role of bile salts in digestion, *Adv. Colloid Interface Sci.*, 2011, **165**, 36–46.

23 F. J. Alvarez and V. J. Stella, The Role of Calcium Ions and Bile Salts on the Pancreatic Lipase-Catalyzed Hydrolysis of Triglyceride Emulsions Stabilized with Lecithin, *Pharm. Res.*, 1989, **6**, 449–457.

24 A. Alayoubi, M. S. Aqueel, C. N. Cruz, M. Ashraf and A. S. Zidan, Application of *in vitro* lipolysis for the development of oral self-emulsified delivery system of nimodipine, *Int. J. Pharm.*, 2018, **553**, 441–453.

25 J. Teixé-Roig, G. Oms-Oliu, I. Odriozola-Serrano and O. Martín-Belloso, Enhancing *in vivo* retinol bioavailability by incorporating β-carotene from alga Dunaliella salina into nanoemulsions containing natural-based emulsifiers, *Food Res. Int.*, 2023, **164**, 112359.

26 E. Troncoso, J. M. Aguilera and D. J. McClements, Fabrication, characterization and lipase digestibility of food-grade nanoemulsions, *Food Hydrocolloids*, 2012, **27**, 355–363.

27 M. J. Dille, T. Baydin, K. A. Kristiansen and K. I. Draget, The impact of emulsion droplet size on *in vitro* lipolysis rate and *in vivo* plasma uptake kinetics of triglycerides and vitamin D 3 in rats, *Food Funct.*, 2021, **12**, 3219–3232.

28 L. Salvia-Trujillo, C. Qian, O. Martín-Belloso and D. J. McClements, Influence of particle size on lipid digestion and β-carotene bioaccessibility in emulsions and nanoemulsions, *Food Chem.*, 2013, DOI: 10.1016/j.foodchem.2013.03.050.

29 A. Torcello-Gómez and T. J. Foster, Instant polysaccharide-based emulsions: impact of microstructure on lipolysis, *Food Funct.*, 2017, **8**, 2231–2242.

30 N. Scheuble, A. Iles, R. C. R. Wootton, E. J. Windhab, P. Fischer and K. S. Elvira, Microfluidic Technique for the Simultaneous Quantification of Emulsion Instabilities and Lipid Digestion Kinetics, *Anal. Chem.*, 2017, **89**, 9116–9123.

31 A. Sarkar, D. S. Horne and H. Singh, Pancreatin-induced coalescence of oil-in-water emulsions in an *in vitro* duodenal model, *Int. Dairy J.*, 2010, **20**, 589–597.

32 T. M. Giang, S. Le Feunteun, S. Gaucel, P. Brestaz, M. Anton, A. Meynier and I. C. Trelea, Dynamic modeling

33 highlights the major impact of droplet coalescence on the *in vitro* digestion kinetics of a whey protein stabilized sub-micron emulsion, *Food Hydrocolloids*, 2015, **43**, 66–72.

33 Y. Li and D. J. Mcclements, New mathematical model for interpreting ph-stat digestion profiles: Impact of lipid droplet characteristics on *in vitro* digestibility, *J. Agric. Food Chem.*, 2010, **58**, 8085–8092.

34 S. H. E. Verkempinck, J. M. Guevara-zambrano, M. R. Infantes-garcia and M. C. Naranjo, Gastric and small intestinal lipid digestion kinetics as affected by the gradual addition of lipases and bile salts, *Food Biosci.*, 2022, **46**, 101595.

35 P. K. Okuro, M. Viau, S. Marze, S. Laurent, R. L. Cunha, C. Berton-Carabin and A. Meynier, *In vitro* digestion of high-lipid emulsions: towards a critical interpretation of lipolysis, *Food Funct.*, 2023, **14**, 10868–10881.

36 Y. E. Arnold, G. Imanidis and M. Kuentz, Study of drug concentration effects on *in vitro* lipolysis kinetics in medium-chain triglycerides by considering oil viscosity and surface tension, *Eur. J. Pharm. Sci.*, 2011, **44**, 351–358.

37 A. Ye, J. Cui, X. Zhu and H. Singh, Effect of calcium on the kinetics of free fatty acid release during *in vitro* lipid digestion in model emulsions, *Food Chem.*, 2013, **139**, 681–688.

38 H. Y. Eldemnawy, A. Wright and M. Corredig, A Better Understanding of the Factors Affecting *In vitro* Lipolysis Using Static Mono-compartmental Models, *Food Dig.*, 2015, **6**, 10–18.

39 S. H. E. Verkempinck, L. Salvia-Trujillo, M. I. Garcia, M. E. Hendrickx and T. Grauwet, From single to multire-sponse modelling of food digestion kinetics: The case of lipid digestion, *J. Food Eng.*, 2019, **260**, 40–49.

40 M. Mazumdar, A. S. Jammoria and S. Roy, Effective rates of coalescence in oil–water dispersions under constant shear, *Chem. Eng. Sci.*, 2017, **157**, 255–263.

41 P. Karthik and C. Anandharamakrishnan, Droplet coalescence as a potential marker for physicochemical fate of nanoemulsions during *in vitro* small intestine digestion, *Colloids Surf., A*, 2018, **553**, 278–287.

42 M. N. Corstens, C. C. Berton-Carabin, P. T. Elichiry-Ortiz, K. Hol, F. J. Troost, A. A. M. Masclee and K. Schroën, Emulsion-alginate beads designed to control *in vitro* intestinal lipolysis: Towards appetite-control, *J. Funct. Foods*, 2017, **34**, 319–328.

43 I. Peinado, V. Larrea, A. Heredia and A. Andrés, Lipolysis kinetics of milk-fat catalyzed by an enzymatic supplement under simulated gastrointestinal conditions, *Food Biosci.*, 2018, **23**, 1–8.

44 S. Amara, C. Bourlieu, L. Humbert, D. Rainteau and F. Carrière, Variations in gastrointestinal lipases, pH and bile acid levels with food intake, age and diseases: Possible impact on oral lipid-based drug delivery systems, *Adv. Drug Delivery Rev.*, 2019, **142**, 3–15.

45 B. Bera, R. Khazal and K. Schroën, Coalescence dynamics in oil-in-water emulsions at elevated temperatures, *Sci. Rep.*, 2021, **11**, 1–10.

46 J. Xiao, C. Li and Q. Huang, Kafirin Nanoparticle-Stabilized Pickering Emulsions as Oral Delivery Vehicles:

Physicochemical Stability and *in Vitro* Digestion Profile, *J. Agric. Food Chem.*, 2015, **63**, 10263–10270.

47 T. Krebs, K. Schroën and R. Boom, Coalescence dynamics of surfactant-stabilized emulsions studied with microfluidics, *Soft Matter*, 2012, **8**, 10650–10657.

48 M. R. Infantes-Garcia, S. H. E. Verkempinck, J. M. Guevara-Zambrano, C. Andreoletti, M. E. Hendrickx and T. Grauwet, Enzymatic and chemical conversions taking place during *in vitro* gastric lipid digestion: The effect of emulsion droplet size behavior, *Food Chem.*, 2020, **326**, 126895.